


RESEARCH

Open Access



Phytochemical screening, metabolite profiling and enhanced antimicrobial activities of microalgal crude extracts in co-application with silver nanoparticle

Hanaa Ali Hussein^{1,2}, Desy Fitriya Syamsumir¹, Siti Aisha Mohd Radzi¹, Julius Yong Fu Siong¹, Nor Atikah Mohamed Zin¹ and Mohd Azmuddin Abdullah^{1*} 

Abstract

Background: Microalgae is one of the major sources of natural compounds with antimicrobial activity. The metabolite profiling of the extracts could identify the bioactive compounds based on methanol (MET), ethanol (ETH), chloroform (CHL), hexane (HEX) and water (W) solvent systems. The microalgal crude extracts in co-application with silver nanoparticles (AgNPs) had enhanced antimicrobial activity with potential to overcome the global problem of microbial antibiotic resistance.

Results: *Chlorella* sp. exhibited the highest lipid, *N. oculata* the highest total saturated fatty acids (TSFA), and *T. suecica* the highest mono-unsaturated (MUFA) and poly-unsaturated fatty acids (PUFA). The highest carbohydrate, protein and total phenolics contents (TPCs) were attained by *N. oculata*. The highest total flavonoids contents (TFCs), and chlorophyll *a* and *b* were in *T. suecica*, while comparable level of carotenoids were found in all species. For high-performance thin-layer chromatography (HPTLC) analyses, the eicosapentaenoic acid (EPA) with high peaks were detected in *T. suecica*-HEX and *N. oculata*-CHL; and β -carotene in *Chlorella* sp.-ETH. The gas chromatography–mass spectrometry (GC–MS) analyses showed high 13-docosenamide (Z)- in *T. suecica*-HEX; phytol in *N. oculata*-HEX; and neophytadiene in *Chlorella* sp.-ETH. The AgNPs–MCEs–MET and HEX at the 1.5:1 ratios exhibited strong activities against *Bacillus subtilis*, *Streptococcus uberis*, and *Salmonella* sp.; and the AgNPs–*T. suecica*-HEX and MET and AgNPs–*Chlorella* sp.-HEX at the 1.5:1 ratios exhibited activities against *Klebsiella pneumoniae*.

Conclusion: Different bioactive components were detected in the MCEs based on the HPTLC and GC–MS analyses. Significant antimicrobial activities against the pathogenic microbes were demonstrated by the synergistic effects of the MCEs in co-application with the AgNPs. This could be beneficial in the fight against sensitive and multidrug-resistant bacteria.

Keywords: Microalgae, Solvent systems, Metabolite profiling, Antimicrobial, Silver nanoparticle, Co-application

Introduction

Microalgae could provide a viable molecular pharming system to produce new compounds because of the ease of cultivation and rapid evolution, a short period of time from transition to expansion, and safety aspect as algae do not induce human pathogens, and several strains are generally regarded as safe (GRAS). Microalgae could

*Correspondence: azmuddin@umt.edu.my; joule1602@gmail.com

¹ Institute of Marine Biotechnology, Universiti Malaysia Terengganu, 21030 Kuala Nerus, Terengganu, Malaysia
Full list of author information is available at the end of the article

survive in controlled conditions in the bioreactors for the homogeneity of protein, antibiotics, and phytochemicals synthesis (Jayshree et al. 2016). Among these, *Nannochloropsis* sp., belonging to Eustigmatophyceae, and a unicellular green alga, plays essential role in the food chain system. Rounded in shape, with a diameter of 2–5 μm , *Nannochloropsis* sp. is usually utilized as a live feed in shrimp farms and fish hatcheries (Gwo et al. 2005). *Tetraselmis suecica* (Chlorophyceae), a green marine microalgae, is rich in tocopherols, chlorophylls, and carotenoids (Pérez-lópez et al. 2014). It is also applied in aquacultures as a feed for crustacean larvae and mollusks (Zittelli et al. 2006) or probiotic for fish (Irianto and Austin 2002), or human diets (Carballo-Cárdenas et al. 2003). *Chlorella* sp. is a unicellular photosynthetic microalgae that contains lutein, essential carotenoids such as carotene, and chlorophyll (green photosynthetic pigments) in its chloroplast (Young and Britton 2012). *Chlorella* sp. produces secondary metabolites such as polysaccharides which is a dietary fiber, with specific functions in the human digestive system (Ibañez et al. 2012).

The search for new sources of phytoconstituents such as antioxidants and anti-microbes from microalgae has gained momentum (Maadane et al. 2015; Azim et al. 2018). The microalgal antimicrobial activity is contributed by several bioactive molecules such as fatty acids, terpenes, indoles, acetogenins, volatile halogenated hydrocarbons, and phenols. The antimicrobial effect of *Chaetoceros muelleri* is suggested due to the lipid formation, while the antimicrobial activity of *Dunaliella salina* is attributable to the fatty acids or neophytadiene, α - and β -ionone, β -cyclocitral and phytol (Amaro et al. 2011). For the detection and profiling of these bioactive compounds, the HPTLC is a suitable screening method and essential for routine pharmacokinetics analysis. The main advantage is its capability to analyze multiple samples by utilizing a little amount of mobile phase, resulting in reduced cost of analysis, time, and risk of exposure to toxic organic effluents, thus minimizing the possibility of environmental pollution (Murugesan and Bhuvaneshwari 2016). The GC–MS is also a widely used method, integrating high separation capacity and capillary GC accuracy for complex metabolite profiling, with high level of sensitivity for mass selective detection (Kapoor 2014).

The silver nanoparticles (AgNPs) possess unique electronic, chemical, magnetic and optical characteristics which are different from the bulk metals (Das et al. 2011). The biological synthesis of AgNPs is preferred due to its low cost, high yield, and eco-friendly process, using biological sources such as bacteria, fungi, yeast, virus, algae or plants (Soliman et al. 2018). Green AgNPs have great potentials as cytotoxic agents against

different types of cancer cell-lines (Sunita et al. 2015). The shape of the AgNPs such as spherical, rod-like and triangular shape could influence the antimicrobial activities (Pal et al. 2007). The AgNPs may get involved in the inhibition of protein synthesis by preventing the many translation factors. The strong affinity of the AgNPs towards the thiols group within the proteins may cause the protein chain to unfold leading to protein degradation (Velusamy et al. 2016; Soliman et al. 2018). The combination of AgNPs with sub-lethal concentrations of antibiotics have reportedly significantly improved the cell death and the reactive oxygen species (ROS) production as compared to the antibiotics or AgNPs alone (Gurunathan et al. 2014).

The AgNPs–MCEs co-application has been recently developed as a novel therapeutic formulation to kill cancer cells without affecting the non-cancerous healthy cells (Hussein et al. 2020a, b). The AgNPs–MCEs co-application at the 1.5:1 and 2:1 ratios exhibited cytotoxicity on the breast cancer (MCF-7 and 4T1), but not the non-cancerous (Vero) cells (Hussein et al. 2020a, b). The ratios (1.5:1 and 2:1) were therefore selected for further evaluation on the antimicrobial activities at 500 $\mu\text{g}/\text{mL}$ concentration. The hypothesis of the study is that the effectiveness of the microalgal antimicrobial activities could be enhanced when combined with the AgNPs co-application. The novelty of the study is the formulation of the new antimicrobial agents against different strains of pathogenic bacteria, based on the combination of the MCEs with the AgNPs, which has not been reported before. To our knowledge, there has yet to be any detail analyses of the extraction from different solvent systems, on the chemical compounds of microalgal culture grown over prolonged period, in specific limiting medium such as TMRL. The objectives of this study were to carry out the phytochemical screening, and metabolite profiling of the volatile compounds of the *N. oculata*, *T. suecica*, and *Chlorella* sp. crude extracts (MCEs) from methanol (MET), ethanol (ETH), chloroform (CHL), hexane (HEX) and water (W) solvent systems, using the HPTLC and GC–MS analyses. A new formulation of antimicrobial agents based on the co-application of MCEs with the AgNPs at the correct dosage and ratios, was evaluated.

Materials and methods

Microalgal strains

The *N. oculata*, *T. suecica*, and *Chlorella* sp. were obtained from and identified by Dr. Mohd Fariduddin Othman, from the Fisheries Research Institute of Malaysia, Kuala Muda, Kedah, Malaysia. The partial 18S rRNA sequence, partial rbcL gene, and ITS region showed 97–99% similarity to *N. oculata*, as confirmed by the sequence alignment

and phylogenetic tree analysis, and deposited into the GenBank with accession numbers HQ201714, HQ201713, and HQ201712, respectively (Shah 2014).

Microalgal culture condition and the MCEs preparation

The basic medium, culture conditions and the preparation of the MCEs were as reported earlier (Hussein et al. 2020a, b). The TMRL enrichment medium components were as shown in Additional file 1: Table S1. The cultures were maintained at 28 ± 2 °C, on an orbital shaker (130 rpm) under continuous fluorescence white light. After 14–16 days, the cells were harvested by centrifugation (3500 rpm, 10 min), and dried at 50 °C overnight in an oven, before finally stored at 4 °C until use.

Biosynthesis of AgNPs

The isolation, identification and cultivation of *Lactobacillus plantarum* has been reported (Hussein et al. 2020a, b). The AgNPs biosynthesis was attained by mixing the *L. plantarum* supernatant with 1 mM of silver nitrate (AgNO_3) solution at the 1:1 ratio (v/v), and incubated for 24 h in the dark at 35 °C, 100 rpm. The characterization of the AgNPs has been reported elsewhere (Hussein et al. 2020b), and beyond the scope of current study.

AgNPs–MCEs ratio

The AgNPs (10 mg) were dissolved in 1 mL of dimethylsulfoxide (10 mg/mL stock). Later, 10 mg of the MCEs from different solvent extraction, were mixed with 1 mL of DMSO (10 mg/mL stock). For single applications, 500 µg/mL of each of the AgNPs and MCEs solution were prepared. For the preparation of the co-applications, the AgNPs and MCEs stock solutions each, was mixed to 500 µg/mL concentration, at the 1.5:1 and 2:1 ratios (AgNPs:MCEs, w/w) (Additional file 1: Table S2). Our study on the cytotoxicity of the AgNPs–MCEs co-application has shown that the 1.5:1 and 2:1 ratios exhibit the highest cytotoxicity on the breast cancer cells, but without affecting the Vero cells (Hussein et al. 2020a, b). Hence, the same ratios were evaluated for the effects on the selected bacterial strains.

Determination of lipid, total phenolics, total flavonoids, total carbohydrates, total protein and pigments

Lipid content

After 14–16 days, the cells were harvested by centrifugation (3500 rpm, 10 min). The lipid content was measured using the Bligh and Dyer method (Bligh and Dyer 1959). The sample of 200-mL aliquot was sonicated and centrifuged (3500 rpm, 10 min). The pellet was added into a mixture of distilled water (D.W.), methanol and chloroform (4:10:5 ratios). After 24 h incubation, 5 mL of D.W. and 5 mL of chloroform were added (9:10:10 final ratios)

and then centrifuged. The lipid-containing chloroform layer at the bottom was transferred to a pre-weighed vial using a dropper. The lipid layer was warmed in a water bath (65 °C), until one-third remained, and later oven-dried for 4 h at 80 °C to remove the chloroform and methanol. The lipids were calculated as follows:

$$\text{Lipid content (\%)} = [(w_2 - w_1) / w_d] \times 100, \quad (1)$$

where w_1 is the pre-weighed glass container (g), w_2 is the weight of the lipid content with the glass container (g), and w_d is the dry weight of algal biomass (g).

Fatty acids composition

Lipid of 20 mg was mixed with 2 mL of toluene, followed by 2 mL of 1.5% sulphuric acid in dry methanol and shaken well. The mixture was refluxed for 2 h, and 4 mL of 5% sodium chloride solution was added and the fatty acid methyl esters (FAME) were extracted with hexane. The hexane layer was washed with 2% potassium bicarbonate solution and dried over anhydrous sodium sulphate (Rao et al. 2007; Shah et al. 2016). The FAME were transferred to a vial and injected into GC–MS, to determine its fatty acid composition.

Total phenolics content

The TPC was determined based on the Folin–Ciocalteu method with modifications (Siripatrawan and Harte 2010). The TPC was extracted in methanol/water (80:20) solution. The MCEs of 25 mg was homogenized with methanol/water (3 mL) at 15,000g for 1 min, and then centrifuged further (5000g, 10 min). Later, 100 µL of the MCEs were mixed with D.W (7 mL) and 500 µL of Folin–Ciocalteu reagent (Sigma–Aldrich, USA), and incubated at room temperature (8 min). Then, 900 µL of D.W and 1.5 mL of sodium carbonate was added and incubated at room temperature for 2 h in the dark. A sample of 2 mL was loaded to a 24-well plate in triplicates. The absorbance of the sample was determined at 765 nm using a microplate reader (Thermo Scientific, Varioskan Flash, USA). Quantitative determination of the TPC was performed based on the calibration curve of gallic acid (Sigma, USA) and expressed as gallic acid equivalent (mg/g GAE) by using the equation:

$$y = 0.0106x + 0.0542; R^2 = 0.9995 \quad (2)$$

Total flavonoids content

The TFC was measured according to the aluminium chloride (colorimetric technique) with modifications (Aiyegoro and Okoh 2010). The MCEs sample of 0.1 mL from the stock (10 mg/mL, DMSO) was mixed with methanol (3 mL), 0.2 mL of potassium acetate (1 M) (HmbG

Chemicals, Germany), 200 μL of 10% aluminium chloride (HmbG Chemicals, Germany), and 5.6 mL D.W, and the mixture was kept for 30 min at the room temperature. After incubation, 2 mL from each sample was transferred to the 24-well plate. The absorbance (420 nm) was determined using a Microplate reader (Thermo Scientific, Varioskan Flash, USA). Quantitative determination of the TFC was performed using standard calibration curve of quercetin (QE) (Sigma-Aldrich, USA) at 1 mg/mL, and all the experiments were carried out in triplicate. The TFC was expressed as QE (mg/g) based on the equation:

$$y = 0.03x + 0.04; R^2 = 0.998 \quad (3)$$

Total carbohydrates content

Dried algal biomass of 100 mg was dissolved in 10 mL of 2% sulfuric acid, and autoclaved at 121 $^{\circ}\text{C}$, 20 min. The hydrolyzed sample was mixed with D.W till 100 mL and centrifuged at 2683g (10 min). The supernatant was analyzed for carbohydrates content using the anthrone reagent and glucose standard (System, USA). The reagent (9,10-dihydro-9-oxoanthracene, Sigma, USA) was prepared by mixing anthrone (100 mg) with cold 95% H_2SO_4 (50 mL). Later, 4 mL of the anthrone was mixed with 1 mL of sample and glucose. The mixture was incubated in a boiling water bath (10 min) and left to cool to a room temperature in a desiccator. The mixture (green color) was detected at 630 nm using a microplate reader. The carbohydrate content was measured based on the glucose standard (Guldhe et al. 2016).

Total protein content

The total protein content was determined using the Bradford method. Dried microalgal powder of 10 mg was dissolved in 0.1 mL of 1 M NaOH and incubated in the water bath (80 $^{\circ}\text{C}$, 10 min). Then, 0.9 mL of D.W was mixed with the hydrolyzed mixture, topped up to 1 mL total volume, and centrifuged (12,000g, 10 min). The protein content in the supernatant was measured using bovine serum albumin as the standard (Bio-Rad, USA) (Guldhe et al. 2016).

Pigments

Microalgal powder of 500 mg was dissolved in 10 mL of 80% acetone and centrifuged (3000 rpm, 15 min). The pellet was repeatedly washed with 80% acetone (5 mL), re-centrifuged, until it became colorless. The supernatant was collected and used for pigment quantification (Arnon 1949).

The chlorophyll content absorbance (645 and 663 nm) was measured in a spectrophotometer (UV-1800, Shimadzu, Japan) as follows (Arnon 1949):

$$\text{Chlorophyll } a \text{ } (\mu\text{g/mL}) = 12.7 (A_{663}) - 2.69 (A_{645}), \quad (4)$$

$$\text{Chlorophyll } b \text{ } (\mu\text{g/mL}) = 22.9 (A_{645}) - 4.68 (A_{663}), \quad (5)$$

$$\text{Total chlorophyll } (\mu\text{g/mL}) = 20.2 (A_{645}) + 8.02 (A_{663}), \quad (6)$$

where A = absorbance at the respective wavelength.

The carotenoid content was determined by estimating the same chlorophyll extraction at 480 nm in spectrophotometer (UV-1800, Shimadzu, Japan) as follows (Kirk and Allen 1965):

$$\begin{aligned} \text{Carotenoids } (\mu\text{g/g fresh wt.}) \\ = A_{480} + (0.114 \times A_{663}) - (0.638 \times A_{645}), \end{aligned} \quad (7)$$

where A = absorbance at the respective wavelength.

Metabolite profiling

High-performance thin-layer chromatography (HPTLC)

The HPTLC plates were rinsed with ethanol and later left in the oven for 15 min at 105 $^{\circ}\text{C}$. Ten microlitre of standards (β -carotene and eicosapentaenoic acid (EPA)) and the MCEs solution were spotted on the plate (6 mm bands) by Camag microliter syringe (Hamilton, Bonaduz, GR, Switzerland), with a semiautomatic sampler (ATS4-211117, Camag, Muttenz, Switzerland), on a pre-coated silica gel aluminium plate 60 F-254 (20 \times 10 cm with 250 μm thickness; Merck, Germany). The solvent system consisted of HEX:Ethylacetate (8.5:1.5, v/v). The chromatogram was developed for about 20 min to a height of about 80 mm in a twin-tank chamber Camag Automatic Developing Chamber 2 (ADC2-211246, Camag, Muttenz, Switzerland) previously saturated with the mobile phase.

The images were visualized using the TLC visualizer (Camag-211520, Muttenz, Switzerland) with a 12-bit charge-coupled device (CCD) digital camera and Win CATS software (Camag, Muttenz, Switzerland) under 366 nm UV and white light. The plates were placed in the dark for 30 min and the images were taken before and after the derivatization with anisaldehyde reagent (Sigma-Aldrich, Germany). The anisaldehyde reagent was prepared by mixing methanol (85 mL), acetic acid (10 mL), methoxy benzaldehyde (0.5 mL) and sulfuric acid (5 mL) (Kowalska and Sherma 2006). The Win CATS image capturing parameters were fixed for high quality and reproducibility. After derivatization, the plates were scanned (Camag TLC Scanner) at 569 nm, 20 mm/s scanning speed and the slit dimension of 4 \times 0.45 mm. The peak list, width, and densitogram were recorded (Chaudhari et al. 2006; Alam 2013). The identification of β -carotene and EPA in the standards and the MCEs was based on the

retention factor (R_f) value as determined by Win CATS software (Camag, Muttenz, Switzerland).

Gas chromatography–mass spectrometry (GC–MS)

The GC–MS analyses were carried out based on simple modification of the previous method (Phuong et al., 2018). The MCEs of 1 mg dissolved in 1 mL hexane was injected into the GC with a capillary column (0.25 mm i.d \times 30 m, 0.25 μ m film thickness) (GCMS QP2010 Ultra, Shimadzu SH-Rxi-5Sil MS, Shimadzu, USA). The conditions were as follows: the injector and the interface at 250 °C; the column in a programmed mode at 50 °C initial temperature, held for 2 min with a linear ramp of 10 °C/min, until 230 °C final temperature. The carrier gas was helium (4.6 mL/min) at the 1:0 split ratio and the sample volume injected was 1 μ L. The mass spectra of the molecules were confirmed and identified with the database in the NIST mass spectral library.

Antimicrobial activity assay

The antimicrobial activities assay was carried out using agar well diffusion method on pathogenic multi-drug resistant bacteria of Gram-positive (*Bacillus subtilis*, *Streptococcus uberis*) and Gram-negative (*Klebsiella pneumoniae*, *Salmonella* sp.). These bacterial strains are the major microorganisms that contaminate and cause damage to the food. The contamination of the food products by these bacteria has led to food poisoning and health hazards (Rajeshkumar and Malarkodi 2014). The bacterial culture collection was established in the Institute of Marine Biotechnology, Universiti Malaysia Terengganu. Standardized suspension of tested bacteria (1.5×10^8 CFU/mL) by McFarland standard (0.5 N) was swabbed on sterile Muller–Hinton Agar (MHA) plates using sterilized cotton swabs. The agar was perforated with a sterilized cork borer (6 mm). A 100- μ L sample from the AgNPs and MCEs (500 μ g/mL) single and co-application at the 1.5:1 and 2:1 (w/w) ratios were added into each well. The concentration of the penicillin (PC) (Oxoid, UK) evaluated was at 10 μ g/disc, following the manufacturer's protocol and also as reported earlier (Pengov and Ceru 2003). One petri dish was sub-cultured with each pathogenic bacteria, or used as control, and incubated at 37 °C for 24 h. Then, the inhibition zone was observed and determined for analysis against each type of test microorganism (Rajeshkumar and Malarkodi 2014).

The microtiter plate dilution method was used to determine the minimum inhibitory concentration (MIC) of the extracts. Sterile 96-well microplates (Nunc) were used for the assay. The extracts were dissolved in DMSO so that the final concentrations in the micro-wells were less than 1% DMSO and the solvent controls were tested

at these concentrations. The MCEs were prepared at the following concentrations—1.95, 3.91, 7.81, 15.62, 31.25, 62.5, 125, 250 and 500 μ g/mL, and 1% DMSO was used as the solvent control. The MCEs or AgNPs or the co-applications were diluted to twice the desired initial test concentration (500 μ g/mL) with Muller–Hinton broth (MHB). All wells, except the first, were filled with MHB (50 μ L). The extracts (100 μ L) were added to the first well and serial twofold dilutions were made down to the desired minimum concentration (2 μ g/mL). An overnight culture of the bacteria suspended in MHB was adjusted to the turbidity equal to 0.5 McFarland standards. The plates were inoculated with the bacterial suspension (5 μ L/well) and incubated at 37 °C for 24 h. Then, the turbidity was measured using micro-plate reader (Biotek) at 620 nm wavelength (Talib et al. 2012).

Statistical analyses

The analyses were carried out for the means of triplicates \pm standard deviation, and the significance was evaluated based on the ANOVA model, Turkey's tests (GraphPad Prism, version 6, CA, USA). The $p < 0.05$ was considered to evaluate the significance of differences.

Results

Phytochemical screening

Lipid, fatty acids, total carbohydrates and total protein contents

The lipid contents in *Chlorella* sp. was the highest (Table 1), followed by *N. oculata*, and *T. suecica*. These were all achieved in the nutrient-limiting TMRL culture media. The highest carbohydrate and protein contents were shown, respectively, by *N. oculata* (17%, 9.6%), followed by *T. suecica* (16.9%, 8.7%), and *Chlorella* sp. (15.5%, 6.9%). There were no significant differences between *N. oculata* and *T. suecica* in their carbohydrate content ($p > 0.05$), while for total lipids and protein, there were significant differences between all algal species ($p < 0.05$). Table 2 shows that the total saturated fatty acids (TSFA) was the highest in *N. oculata*, followed by *Chlorella* sp. while both mono-unsaturated fatty acids (MUFA) and poly-unsaturated fatty acids (PUFA) were the highest in *T. suecica*, followed by *Chlorella* sp. Pentadecanoic acid, C15:0 and stearic acid, C18:0 were only detected in *N. oculata*; linoleic acid, C18:2n6C only in *T. suecica*; and palmitic acid, C16:0 only in *Chlorella* sp. The highest fatty acids component detected in *N. oculata* and *Chlorella* sp. was tricosylic acid, C23:0 (41.02, 38.39%, respectively), and nervonic acid, C24:1 (36.38%) in *T. suecica*. Both *Chlorella* sp. and *T. suecica* showed great potential as the sources of EPA and nervonic acid for nutraceutical applications.

Table 1 Lipid (%), measured using the Bligh and Dyer method), carbohydrate (%), measured using anthrone reagent and glucose as standard), protein (%), measured using Bradford method and bovine serum albumin as standard), total phenolic content (TPC, expressed as gallic acid equivalent (mg/g GAE)) and total flavonoids content (TFC, expressed as quercetin (mg/g)) of microalgae crude extracts (MCEs)

Microalgae species	Lipid (%)	Total carbohydrate (%)	Total protein (%)	TPC, mg/g Gallic acid equivalent (GAE)					TFC, mg/g Quercetin equivalent (QE)				
				Methanol	Chloroform	Hexane	Ethanol	Water	Methanol	Chloroform	Hexane	Ethanol	Water
<i>N. oculata</i>	23.7 a ± 0.99	17 a ± 0.01	9.6 a ± 0.05	58.1 a ± 0.042	24.5 b ± 0.01	7.1 c ± 0.01	13.6 d ± 0.01	5.8 e ± 0.06	44.83 a ± 0.04	22.5 b ± 0.002	14.7 c ± 0.02	10.9 d ± 0.001	5.9 e ± 0.001
<i>T. suecica</i>	15.9 b ± 0.76	16.9 a ± 0.01	8.7 b ± 0.06	44.3 a ± 0.032	1.70 b ± 0.01	0.8 c ± 0.001	15.2 d ± 0.001	7.1 e ± 0.06	97.67 a ± 0.07	25.7 b ± 0.003	1.0 c ± 0.001	15.5 d ± 0.01	9.9 e ± 0.02
<i>Chlorella</i> sp.	30.38 c ± 0.92	15.5 b ± 0.01	6.9 c ± 0.07	35.7 a ± 0.031	5.94 b ± 0.02	0.7 c ± 0.01	17.4 d ± 0.001	5.9 e ± 0.06	55.84 a ± 0.062	39.1 b ± 0.004	1.38 c ± 0.06	17.3 d ± 0.001	2.2 e ± 0.02

Values are expressed as mean ± standard deviation, *n* = 3; TPC total phenolic content, TFC total flavonoid content

For lipids, carbohydrate and protein, for each column, different letters indicate significantly different (*p* < 0.05)

For TPC and TFC, a–e values in the same line sharing different letters are significantly different (*p* < 0.05)

Table 2 The major fatty acids constituent of *N. oculata*, *T. suecica* and *Chlorella* sp. grown in TMRL media at 28 ± 2 °C

Microalgae/fatty acids	<i>N. oculata</i> (%)	<i>T. suecica</i> (%)	<i>Chlorella</i> sp. (%)
TSFA	71.25	23.11	42.02
MUFA	20.29	37.38	35.19
PUFA	8.48	30.5	22.8
Pentadecanoic acid, C15:0	7.47		
Palmitic acid, C16:0			3.63
Stearic acid, C18:0	17.47		
Linoleic acid, C18:2N6C		29.19	
Eicosapentaenoic acid (EPA, timnodonic acid), C20:5N3	8.48	11.31	20.48
Tricosylic acid, C23:0	41.02	21.25	38.39
Nervonic acid, C24:1	19.74	36.38	33.5

TPC, TFC, total carotenoids and chlorophyll

The TPC and TFC are shown in Table 1. *Chlorella* sp.-CHL exhibited the highest TPC (mg/g GAE), followed by *N. oculata*-MET and *T. suecica*-MET, *Chlorella* sp.-MET, *N. oculata*-CHL and *T. suecica*-CHL. The MET and CHL were more suitable for TPC extraction than HEX, ETH and W. The TPC of *Tetraselmis* sp.-MET in our study was higher than the reported values of 16.868 mg/g GAE (Widowati et al. 2017); 3.8 mg/g GAE extract (Goiris et al. 2012); and 25.5 ± 1.5 mg/g GAE ethanolic extracts (Maadane et al. 2015). For TFCs analyses (mg/g QE), MET was proven as the superior solvent, as exhibited by *T. suecica*-MET (97.7), *Chlorella* sp.-MET (55.8) and *N. oculata*-MET (44.8), followed by the MCEs-CHL (22.5–39.1 mg/g QE). The TPC and TFC contents were significantly different between algal species ($p < 0.05$). *Chlorella* sp. showed a comparable level of carotenoids with *N. oculata* and *T. suecica*. The highest chlorophyll *a* and *b* were shown, respectively, by the *T. suecica* (30.72, 60.14 $\mu\text{g}/\text{mL}$), followed by *N. oculata* (30.32, 58.97 $\mu\text{g}/\text{mL}$) and *Chlorella* sp. (27.70, 26.9 $\mu\text{g}/\text{mL}$) (Table 3).

Metabolite profiling of MCEs

HPTLC

The HPTLC analyses facilitate the repeated capture of the chromatograms from the same or different samples

Table 3 The pigment composition of *N. oculata*, *T. suecica* and *Chlorella* sp. obtained by extraction with 80% acetone and determined by spectrophotometer at absorbance 480, 663, 645 nm

Microalgae	Chlorophyll <i>a</i> ($\mu\text{g}/\text{mL}$)	Chlorophyll <i>b</i> ($\mu\text{g}/\text{mL}$)	Total Chlorophyll ($\mu\text{g}/\text{mL}$)	Carotenoid ($\mu\text{g}/\text{g.fr.wt}$)
<i>N. oculata</i>	30.32 a	58.97 a	89.34 a	2.30 a
<i>T. suecica</i>	30.72 a	60.14 b	90.83 a	2.27 a
<i>Chlorella</i> sp.	27.70 b	26.9 c	54.59 b	2.31 a

Each column with the same letters indicate not significantly different at $p > 0.05$

(Sushma et al. 2013; Pandithurai et al. 2015; Murugesan and Bhuvanewari 2016). It is therefore suitable for the development of chromatographic fingerprints to detect the main active compounds in microalgae. The resolution and separation are much better, and the results are more dependable and versatile than the TLC. In combination with digital scanning profiling, the HPTLC provides quantitative measurement by scanning densitometry which is suitable to evaluate the therapeutic effectiveness of the drug as well as in the identification, standardization, and quality control of the experimental algae (Thenarasan et al. 2014). The plate was visualized under the white light, 254 nm, 366 nm and the derivatized plates by anisaldehyde staining. The standard compounds, EPA and β -carotene, were observed in all extracts but the intensities were different between species, and between extracts for the same species. Additional file 1: Fig. S1 shows that the most intense peaks and better separation of the standard compounds were based on the solvent system hexane:ethylacetate (8.5:1.5 v/v). The ETH showed more separation of compounds, followed by CHL and HEX extracts. However, the MET and W extracts did not exhibit any standards within the sample using the same solvent system. For the standard bands, the ETH also exhibited higher intensity for all MCEs, followed by the CHL and HEX. The lower intensity of β -carotene in HEX extracts could possibly because of the exposure to direct heat and light (Hynstova et al. 2017).

To confirm the absence or presence of standards in the MCEs, the HPTLC dimensional fingerprint was obtained by scanning the plate using the TLC scanner as exhibited in the HPTLC chromatogram (Additional file 1: Figs. S2–S4). The scanning technique was a reliable, fast and accurate tool for the identification of standards in the tested sample and profiles in the marine algal extracts based on the peaks, R_f values, and the areas. The chromatographic fingerprints detected, such as in the *Spatoglossum*

asperum, may be saved as electronic images without any errors and changes, allowing for more in-depth investigation (Pandithurai et al. 2015). Additional file 1: Tables S3–S5 show the R_f values and the peak area to indicate the specific differences of compounds in the MCEs. The R_f values of EPA and β -carotene in the CHL, HEX and ETH were comparable. The peak area differences were however showing greater differences [CHL, (41.59, 26.67%); HEX, (67.78, 11.74%); and ETH, (73.79, 33.49%)], respectively. Within microalgal samples, the R_f values of EPA and β -carotene in CHL extracts were also comparable but greater differences were observed for the peak area [*N. oculata*, (22.69, 28.27%); *T. suecica*, (15.66, 15.03%); and *Chlorella* sp. (10.76, 15.71%)], respectively. The HEX extracts showed the presence of EPA and β -carotene within the microalgal sample, with greater differences of the R_f values [(0.48, 0.72), (0.44, 0.71) and (0.49, 0.72)], and the peak [(21.04, 19.96%), (26.73, 29.71%) and (21.02, 15.56%)] for, respectively, *N. oculata*, *T. suecica*, and *Chlorella* sp. The ETH extracts showed the presence of EPA and β -carotene with more distinct R_f [(0.59, 0.74), (0.6, 0.73) and (0.63, 0.73)], and the area [(25.02, 10.59%), (11.46, 12.45%), and (14.86, 16.20%)], respectively, with higher area of EPA for *N. oculata*, and higher β -carotene for *Chlorella* sp.

GC-MS

Table 4 shows the peak area (%) and retention time (R_t) of the major compounds in MCEs-MET, HEX and ETH extracts. For MET extracts, the major compounds in *N. oculata*-MET and *T. suecica*-MET were 13-docosenamide, (Z)- and 9,12,15-octadecatrienoic acid, methyl ester, (Z,Z,Z), while in *Chlorella* sp. was diisooctyl phthalate. The ETH extracts exhibited the presence of 11 compounds considered as major. Neophytadiene (19.81%) was detected in *Chlorella* sp.-ETH, 13-docosenamide, (Z)- (17.46%) in *N. oculata*-ETH, neophytadiene (13.57) and ergost-5-en-3-ol, (3 beta)- (12.33%) in *T. suecica*-ETH and 9,12,15-octadecatrienoic acid, (Z,Z,Z)- (12.08%) in *N. oculata*-ETH. The presence of diethyl phthalate, *n*-hexadecanoic acid, phytol, heptasiloxane, hexadecamethyl-, cyclononasiloxane, octadecamethyl-, 1-nadecene, and *n*-tetracosanol-1 were between 0.2 and 11.3%.

The HEX extracts exhibited 9 compounds identified as major—13-docosenamide, (Z)- (48.36%) in *T. suecica*-HEX, phytol (29.49%) in *N. oculata*, and ergost-7-en-3-ol (16.58 and 14.30%) in *Chlorella* sp.-HEX and *N. oculata*-HEX, respectively. The presence of neophytadiene, 1,2-benzenedicarboxylic acid, bis (2-methylpropyl) ester, vitamin E, diisooctyl phthalate, phenol, 2,2'-methylenebis [6-(1,1-dimethylethyl)-4-methyl- and eicosane were also detected. In comparison, the CHL extracts showed 11

major compounds including hexanedioic acid, bis (2-ethylhexyl) ester, eicosane, neophytadiene, and tetracontane. The major compounds in *T. suecica*-CHL were tetracontane, eicosane, hexatriacontane, hexanedioic acid, bis (2-ethylhexyl) ester, and neophytadiene (Hussein et al. 2020a), while in *N. oculata*-CHL and *Chlorella* sp.-CHL were hexanedioic acid, bis (2-ethylhexyl) ester, neophytadiene, eicosane, hexatriacontane and 13-Docosenamide, (Z) (Hussein et al. 2020b). There was no phytol, tetracontane, 13-docosenamide, (Z), vitamin E and campesterol detected in *N. oculata*-CHL; diisooctyl phthalate and vitamin E were absent in *T. suecica*-CHL; and hexatriacontane was absent in both *T. suecica*-CHL and *Chlorella* sp.-CHL (Hussein et al. 2020a, b). The major metabolites in the MCEs based on the five solvent were therefore 13-docosenamide, (Z)- in *T. suecica*-HEX (48.39%); hexanedioic acid, bis (2-ethylhexyl) ester (36.47%) and Phytol (29.49%) in *N. oculata*-CHL and HEX, respectively; hexanedioic acid, bis (2-ethylhexyl) ester (23.94%) in *Chlorella* sp.-CHL and neophytadiene (19.81%) in *Chlorella* sp.-ETH. The GC-MS could not be carried out on the W extract as it could not be dissolved in the *n*-hexane solvent.

Antimicrobial activities

The antimicrobial activity or inhibition zones of the AgNPs and MCEs (500 μ g/mL) single application was observed against most of the pathogenic bacteria studied (Fig. 1, Additional file 1: Tables S6, S7). The inhibition zones (Additional file 1: Figs S5–S8) obtained indicate the strength of the antimicrobial activity of the sample. The AgNPs showed the highest activity (inhibition zone) of 19, 19, 18 and 23 mm on *B. subtilis*, *S. uberis*, *Salmonella* sp. and *K. pneumoniae*, respectively. The antimicrobial activity of the MCEs was significantly affected by the different solvents used for the extraction ($p < 0.05$). *N. oculata*-CHL exhibited the highest activity against *S. uberis* and *K. pneumoniae*. Both *T. suecica* and *Chlorella* sp. from all solvent extracts, except for ETH, also showed activities against *K. pneumoniae*. The PC and the *N. oculata*-MET however had no activities against *K. pneumoniae*, although the *N. oculata*-MET actually exhibited activities against Gram-positive (G^{+ve}) bacteria (12–14 mm) and also *Salmonella* sp. The G^{+ve} bacteria lacks the outer membrane components, but the presence of thicker cell wall with peptidoglycan layer may affect the access to the extracts and the PC. The *Chlorella* sp.-MET and CHL exhibited activities against the Gram-negative (G^{-ve}) bacteria (11–14 mm). The *Chlorella* sp. and *T. suecica*-CHL exhibited the highest activity against *K. pneumoniae* and *S. uberis*, respectively, while the ETH and W extracts exhibited the lowest activity against *Salmonella* sp. as compared to the other

Table 4 Metabolites of the MCEs from different solvent systems and their respective retention times obtained by GC-MS

Compounds	Rt (min)	HEX		MET		ETH					
		N. oculata		Chlorella sp.		Chlorella sp.		N. oculata			
		(%)	(%)	(%)	(%)	(%)	(%)	(%)	(%)		
Fatty acid											
Tetradecanoic acid	29.26			1.06	0.76	2.41		5.73	9.75	3.83	
<i>n</i> -Hexadecanoic acid	33.6							12.08			
9,12,15-Octadecatrienoic acid, (Z,Z,Z)-	37.1							3.73		10.74	
1-Nonadecene	34.2								1.26	6.76	
<i>n</i> -Tetracosanol-1	38.1										
Ergost-7-en-3-ol	55.7	2.12	14.30	16.58							
Ergost-5-en-3-ol, (3.β,24r)-	54.7								12.33		
Alkane											
Eicosane	43.4	3.55	2.67	1.56							
Ester											
9,12-Octadecadienoic acid, methyl ester	32.07			4.22		1.58					
7,10,13-Hexadecatrienoic acid, methyl ester	32.17			5.59	0.48	1.52					
Hexadecanoic acid, methyl ester	32.79			5.55	10.92	6.75					
9,12,15-Octadecatrienoic acid, methyl ester, (Z,Z,Z)	36.3			16.83	13.23	7.34					
Diisooctyl phthalate	43.90	2.23	4.15	2.73	6.97	12.43					
1,2-Benzenedicarboxylic acid, bis (2-methylpropyl) ester	31.4		0.26	12.41							
Diethyl Phthalate	25.1							3.40	5.68	2.79	
Phenol											
2,4-Di-tert butylphenol	23.1			4.06	1.2	0.98					
Cont. Phenol, 2,2'-methylenebis[6-(1,1-dimethylethyl)-4-methyl-]	41.8	6.69		1.69							
Terpene											
Neophytadiene	30.9	1.77	0.42	11.28	4.4	6.99		9.24	13.57	19.81	
Phytol	36.5	29.49	8.18	14.55				8.73	8.40	6.82	
Amide group											
13-Docosenamide,(Z)-	47.7	1.62	48.39	17.79	16.01			17.46	9.62		
Vitamin											
Vitamin E	52.7	1.74									
Others											
Benzenamine, 4-octyl-N-(4-octylphenyl)-	50.3			8.13	1.94	5.27					
Heptasiloxane, hexadecamethyl-	38.2							4.12	11.3		
Cyclonasiloxane, octadecamethyl-	45.02							5.77	8.94		

MCEs. Additional file 1: Table S8 shows that the MIC of the MCEs and AgNPs single application varied. The MIC of the AgNPs was 15.62 µg/mL against *K. pneumoniae*, and 31.25 µg/mL against *B. subtilis*, *S. uberis*, and *Salmonella* sp. The MIC of the MCEs-MET, CHL, HEX, ETH and W were at 62.5–125 µg/mL against all the tested bacteria, while the MIC of PC were lower against *B. subtilis* and *S. uberis*, and 62.5 µg/mL against *Salmonella* sp. For the AgNPs–MCEs co-application, the MIC on average ranged between 31.25 and 62.5 µg/mL (Additional file 1: Table S9) which was better than the MCEs single application. The co-application exhibited more consistent and enhanced antimicrobial activities against all the pathogenic bacteria. The activities of all the MCEs were therefore improved in co-application with the AgNPs at the 1.5:1 and 2:1 ratios.

The antimicrobial activities of the AgNPs–MCEs co-application were significantly affected by the different solvents used for the extraction, the AgNPs-to-MCEs ratios, and the microalgal species ($p < 0.05$) (Fig. 1). The AgNPs–*Chlorella* sp.-MET and AgNPs–*T. suecica*-MET and HEX showed enhanced activity at the 1.5:1 ratio (10–16 mm), higher than the 2:1 ratio (8–15 mm). For G^{+ve} bacteria, the increased activities against *B. subtilis* and *S. uberis* were detected with the AgNPs–*T. suecica* and AgNPs–*Chlorella* sp.-MET (1.5:1) (from no activity to 16 and 15 mm, respectively), and the AgNPs–MCEs–CHL

and HEX also showed improved activities. For the G^{-ve} bacteria, the AgNPs–*N. oculata*-MET (1.5:1) showed significant increase in activity (16 mm), followed by AgNPs–*T. suecica*-MET against *Samonella* sp.; and the AgNPs–*N. oculata*-W (1.5:1) and AgNPs–*T.suecica*-HEX (1.5:1) against *K. pneumoniae*. The AgNPs–*Chlorella* sp.-MET (1.5:1) also exhibited high activities against *Salmonella* sp. and *K. pneumoniae*. The presence of AgNPs therefore increased the sensitivity of all the bacterial strains to the MCEs as compared to the single application.

Discussion

The TMRL medium contained only basic macro/micro-nutrients, which may lead to a decrease in cell density and growth rate. The medium composition and reactor configuration play important roles in determining the level of cell growth or production of bioactive compounds in microalgae. In a study, three constituents of TMRL enrichment medium (KNO_3 , Na_2HPO_4 and $FeCl_3$) have been modified with excess level to stimulate cell growth, and reduced level to simulate stress conditions to enhance the metabolites production (Shah and Abdullah 2018). In Conway media, *Chlorella* sp. achieves the highest lipid content of 30% after 2 weeks, and 26.8% after

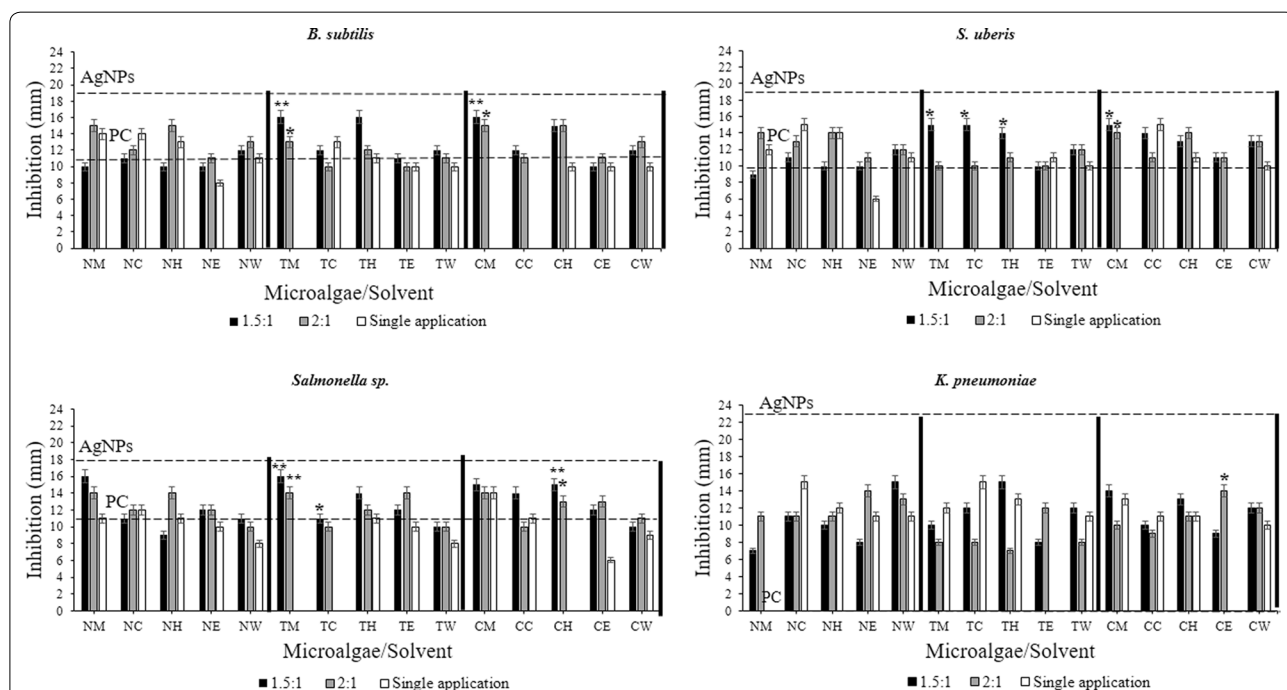


Fig. 1 Inhibitory effects (mm) of AgNPs and MCEs (500 µg/mL) single and co-application at the 1.5:1 and 2:1 ratio on selected microorganisms for 24 h by using well diffusion methods. The results are expressed as the mean ± SD, each of which contained three replicates. The horizontal dashed lines indicate the inhibitory zones of AgNPs and PC (N–*N. oculata*; T–*T. suecica*; C–*Chlorella*; M–methanol; C–chloroform; H–hexane; E–ethanol; W–water)

16 days (Ahmad et al. 2014), as compared to *N. oculata* at 23.5% and 20.8%, respectively (Ahmad et al. 2015). Different studies have reported *N. oculata* having lipid levels between 22.7 and 29.7%, *T. suecica* between 8.5 and 23%, and *Chlorella* sp. between 5 and 58% (Mata et al. 2010), and as low as 2.5% of dry weight for *T. suecica* (Servel et al. 1994). The variation, the type and the total content in the fatty acid components may suggest the effects of nutrient limitation (Arisz et al. 2000) which are species-specific, influenced by factors such as the duration and cultivation conditions including the salinity, light intensity, temperature, pH, the culture medium used and the concentration of nitrogen and other nutrients (Gouveia and Oliveira 2009; Gu et al. 2012; Abdullah et al. 2016; Safafar et al. 2016). In our study, the use of TMRL medium is for the purpose of inducing the secondary metabolites production in microalgae when grown under stressed conditions over prolonged period of cultivation, and to evaluate the effects of the compound induction in the extracts on the cytotoxic (Hussein et al. 2020a; b) and antibacterial activities.

The content of polar lipids could decrease with the culture age (Rao et al. 2007), while the accumulation of SFA and MUFA may be influenced by the nitrogen level. A reduction in nitrogen concentration has led to improved phospholipids from about 6 to 8%, and the non-polar lipids from 73 to 79%, whilst the fraction of galactosylglycerides decrease from 21 to 12% (Alonso et al. 2000). Some of the fatty acids are important in retaining the permeability-barrier, and may be useful in skin treatment (Servel et al. 1994). The *N. oculata* and *T. suecica* grown in 10% palm oil mill effluent (POME) in sea water media attain, respectively, different levels of TSFA (59.2, 68.7%), MUFA (15.1, 12.3%) and PUFA (9.1, 8.9%) (Shah et al. 2016). Other study has reported the SFA, MUFA, and PUFA of 27.5, 30 and 42.3% for *Nannochloropsis* sp., and 23.2, 14.9 and 62.1% for *Chlorella* sp., respectively (Yao et al. 2015). *Chlorella* contains the highest amount of total MUFA and PUFA and rich in C18:3 (21%), C18:1c (9%), C16:3 (13%), C16:0 (20%), and C18:2 (23%), accounting for 86% of the overall fatty acids. *Nannochloropsis* sp. has the highest *n*-3 fatty acids (37%) and rich in C20:5 (30%), C14:0 (6%), C20:4 (6%), C16:1 (24%), and C16:0 (19%), accounting for 85% of the total fatty acids (Yao et al. 2015).

Both carbohydrate and protein are also important components in microalgae. In contrast to our study, *N. oculata* has reportedly achieved lower carbohydrates content of around 7–8%, but higher protein around 35% (Brown 1991), and 21% (Hafsa et al. 2017). When grown at 25 °C, the carbohydrates in *N. oculata* are reportedly high at 29.4% (Picardo et al. 2013). For *Chlorella* cultures grown in BBM Medium, low total carbohydrate

(41.09 mg/g) and protein content (34.56 mg/g) on dry biomass basis have been reported (Dineshkumar et al. 2017). In some algal species, it is difficult to measure the total protein content due to the presence of tough cell walls that are difficult to break (Servaites et al. 2012). Protein may constitute up to 50% or more of the total biomass (Becker 2007), and if protein is the target bioactive compound, an increase in nitrogen in the medium is essential (Safafar et al. 2016). Different levels of chlorophyll *a* and *b* contents have been reported, respectively, in *Chlorella* sp. (8.45, 4.33 µg/mL), and *Nannochloropsis* (21.24, 9.66 µg/mL) (Oo et al. 2017), and *C. vulgaris* (502, 71.9 µg/g cell) (Gonzalez and Bashan 2000). The differences in pigment level of microalgal species living in the same environment can be attributed to the light stratification. The exposure of chlorophyll molecules to light, oxygen or weak acids will accelerate oxidation, leading to the formation of many by-products (Humphrey 1980; Jeffrey et al. 1997; Cubas et al. 2008). Apart from light stratification, the lower chlorophyll level can be due to the effect of temperature (Dere et al. 1998). In addition, the non-conservative nutrients in culture media such as nitrate and phosphate and solvents for extraction can influence the yield and the level of chlorophyll content (Oo et al. 2017).

The phenol extraction in ethanol and other organic solvents is reportedly higher than water (Wang et al. 2009; Farvin and Jacobsen 2013). The TPC (mg/g GAE D.W.) in ethanol/water extracts from *Chlorella* sp. is between 0.75 and 2.21, *Nannochloropsis* sp. at 1.39 and *T. suecica* at 1.71 (Goiris et al. 2012). The *Chlorella* aqueous extracts achieve the TPC of 1.44 mg/g tannic acid equivalent of algae powder (Wu et al. 2005). The content of non-phenol compounds like terpene and carbohydrate in water extracts however could be more than in other MCEs. This is due to the more complex composition of some phenolic compounds having higher molecular weights or more phenol groups which are soluble in acetone, ethanol, and methanol, than in the water extracts (Do et al. 2014). The levels of TFCs also vary depending on the extracting solvent system and microalgal species. Under copper stress (Cu²⁺), *Tetraselmis* sp. exhibits maximum phenolic content (10.35 ± 0.33 µg/mg GAE extract) while *N. oculata* shows the highest TFC (33.85 ± 3.16 µg/mg QE extract) (Azim et al. 2018). Ethyl acetate extract of *N. oculata* exhibits higher TFC (71.79 ± 2.32 mg/g QE) as compared to the methanol extracts (42.08 ± 1.09 mg/g QE) (Ebrahimzadeh et al. 2018) and higher than the 5.78 mg/g rutin level (Sangeetha et al. 2018). The TFC in *Chlorella pyrenoidosa* (mg/mg of RE equivalent of dry extract) evaluated in heterotrophic and autotrophic modes, respectively, suggests that the water extract exhibits higher TFC (0.6 ± 0.07 and 0.87 ± 0.06 mg/

mg RE), followed by hexane extracts (0.52 ± 0.09 and 0.78 ± 0.07 mg/mg RE) and ethyl acetate extracts (0.50 ± 0.05 and 0.60 ± 0.06 mg/mg RE) (Yadavalli et al. 2018). These are contradictory to our studies that found water and hexane as inefficient solvent systems for TFC and TPC extraction.

The physical and chemical properties of the different metabolic classes served as the basis for the analyses of the organics, sugars, amino acids, lipophilic and sugar alcohols (Alsufyani 2014; Kapoor 2014). The HPTLC analyses of *Spatoglossum asperum* provide typical fingerprints and utilized as a reference to determine and regulate the drug quality. The characterization of the chemical components, the estimation of the marker compounds, and the determination of the standards are all useful in the validation of drug quality control and effective efficacy treatments (Pandithurai et al. 2015). Based on HPTLC analyses, the methanol extracts of marine red alga *Portieri hornemannii* contain a mixture of compounds to provide information about the efficacy of the formulation, as well as identification, standardization and quality control. The pharmacological activities are due to the accumulative effects of all the bioactive compounds (Murugesan and Bhuvanewari 2016). The HPTLC fingerprint of the *Ficus nervosa* chloroform extracts show 11 peaks with R_f ranging from 0.07 to 1; the ethyl acetate extracts with 11 peaks and the R_f values from 0.07 to 0.99, and the 90% ethanol extracts with 13 peaks and the R_f values from 0.03 to 1. The data are useful for the correct recognition of the plants, and as a phytochemical or genetic variability indicator in plant populations (Sushma et al. 2013). The HPTLC analyses have confirmed the presence of more carotenoids and chlorophyll in *C. vulgaris* than in *Spirulina platensis*, with the fastest migratory β -carotene compounds detected in *C. vulgaris* and *S. platensis* (Hynstova et al. 2017).

The GC-MS analyses of the MCEs have detected different volatile and semi-volatile compounds such as phytol, eicosane and neophytadiene, and other studies have reported fucosterol, palmitic, palmitoleic and oleic acids (Alsufyani 2014; Balamurugan et al. 2014; Rajendran et al. 2014). Similar to major compounds detected in our study, different solvent extracts of *Chlorella* sp., *Tetraselmis* sp., *Oscillatoria* sp., *Synechocystis* sp., and *Dunaliella* sp. exhibit the presence of benzoic acid, octadecanoic acid-4-hydroxy-methyl ester, tetradecanoic acid, and hexadecanoic acid (Rajendran et al. 2014). Hexadecanoic acid, tetradecanoic acid and octadecanoic acid methyl ester show anti-bacterial and anti-inflammatory activities (Amarowicz 2009; Al-saif et al. 2014; Swamy and Sinniah 2015), while diisooctyl phthalate exhibits antimicrobial, antibacterial, antifungal, antiviral and antioxidant activities (Phuong et al. 2018). Phytol is a diterpene

which shows anticancer, antimicrobial and antioxidant activities (Wei et al. 2011; Swamy and Sinniah 2015); and antidiuretic, anti-inflammatory, antidiabetic, immunostimulatory, antifungal against *Salmonella typhi*, and antimalarial activities (Balaji et al. 2017). Neophytadiene is also a terpenoid with antimicrobial, antipyretic, anti-inflammatory, analgesic and anti-oxidant activities (Venkara Raman et al. 2012), while stigmasterol, campesterol and ergost-5-en-3-ol are sterols exhibiting anticancer activities. Eicosane is an acyclic alkane, showing antibacterial, antifungal, anticancer and cytotoxic effects (Sunita and Manju 2017), especially against SGC-7901 human gastric cell-lines (Yu et al. 2005; Sivasubramanian and Brindha 2013).

The anti-bacterial activity of the MCEs is contributed by the presence of bioactive constituents such as the lipophilic and phenolic compounds in all organic extracts. The variations are attributable to the thick peptidoglycan layer in G^{+ve} , and the thin peptidoglycan layer surrounded by membrane lipid layer outside the G^{-ve} bacteria (Silhavy et al. 2010; Gurunathan et al. 2014; Otari et al. 2014). The polarity of the extracting solvent profoundly affects the way in which the extract will interact with the functional groups on the bacterial surfaces. The extracted functional groups may be polar hydrophilic or non-polar lipophilic which determine the outcome of the action on the cell membrane and other components of the G^{-ve} and G^{+ve} bacteria (Shannon and Abu-ghannam 2016), and eventually the penetration of the bioactive compounds into the bacterial cells. *N. gaditana* has shown inhibitory activities against *P. aeruginosa*, *S. aureus* and *E. coli* with an MIC of 2.6–4.3 mg/mL which can be correlated to the level of fatty acids, phenolics and carotenoids (Maadane et al. 2017). Higher inhibition zone has been achieved with the methanolic extracts of *Tetraselmis* sp., as compared to diethyl ether and hexane, against *E. coli* (16 mm) and *S. aureus* (15 mm), but all extracts exhibit no activities against *Proteus vulgaris*. The essential compounds suggested to have significant antimicrobial activities are the unsaturated, monounsaturated and saturated fatty acids, halogenated-aliphatic compounds, terpenes, sulphur which include hetero-cyclic compounds, phenols and carbohydrates (Kannan et al. 2010). The lipid compositions of microalgae including the EPA, γ -linolenic, docosahexaenoic, hexadecatrienoic, palmitoleic, oleic, lauric, and arachidonic acids, lactic acid, and the compounds such as α - and β -ionone, β -cyclocitral, neophytadiene, and phytols have exhibited antimicrobial activities against human pathogens including *Staphylococcus epidermidis*, *Pseudomonas aeruginosa*, *S. aureus* and *E. coli* (Smith et al. 2010; Bhattacharjee 2016). The antibacterial and antifungal activities of the microalgal extracts are

attributable to myristic acids (tetradecanoic acid), lauric, stearic (octadecanoic acid), palmitic (hexadecanoic acid), 13-Docosamide, (Z)- oleic, linoleic, and linolenic acids (Agoramoorthy et al. 2007; Kumaradevan et al. 2015).

Microbial source to synthesize the AgNPs has led to the general interest in the recovery of NPs from its metabolic action (Natarajan et al. 2010). The green biosynthesis of the AgNPs is interesting and cost-effective as the reduction of silver ions into the AgNPs are attributed to the presence of the protein molecules and enzymes, including the nitrate reductase in the *L. plantarum* supernatant, that could have acted as the regulating agents (Hussein et al. 2020a, b). The probiotic *Lactobacillus* strains also exhibit antimicrobial and anti-oxidative properties with the abilities to adjust the balance of intestinal flora, reduce the blood cholesterol, inhibit and reduce the risk of tumors and cancer, stimulate the immune system, enhance the digestion and can be utilized for the vitamin C production (Songisepp et al. 2004). As a new generation of antimicrobial agents to overcome the drug resistance of G^{-ve} and G^{+ve} bacteria, the AgNPs–MCEs co-application can be developed as therapeutics, with the AgNPs as adjuvant for the treatment of different diseases caused by the bacteria. The AgNPs–MCEs interaction with the bacterial cells could lead to increased membrane permeability, causing damage, and finally cell death. The differences in the responses of the bacterial strain, even when exposed to the same concentration (500 $\mu\text{g}/\text{mL}$) of the AgNPs–MCEs in our study, suggest the intrinsic sensitivity of the bacterial species. The differential susceptibility between the G^{-ve} and G^{+ve} bacteria to the type of anti-bacterial agent can be attributed to the cell wall components of each bacterial strain, and on the activity of different elements or intrinsic resistome. Resistome provides insights into the antibiotics mode of action and the bacterial response to the inhibition. This inhibition of the functions by the resistant determinants and the hypersensitivity to the antibiotics could have a practical role in determining the targets for the development of co-application drugs to enhance the activity of the existing antibiotics (Blake and O'Neill 2013).

In our study, as shown in Fig. 1 and Additional file 1: Table S6, some of the MCEs did not show any activities. The synergistic effects of the bioactive compounds in the MCEs and the well-reported antibacterial activity of the AgNPs suggest the possibility to adjust the ratios of the AgNPs to the MCEs to enhance the activities against any antibiotic-resistant bacteria. The higher antibacterial activity of the AgNPs–MCEs co-application may be attributed to the bonding reaction of the active compounds of the MCEs with the large surface area of the

AgNPs by chelation (Gurunathan et al. 2014). The AgNPs may be involved in neutralizing the adhesive substances, and get attached to the bacterial cell surface depending on the ratio of the AgNPs to the MCEs. In single application, the AgNPs can be attached directly to the bacteria cells and the antibacterial activities will depend on the level of the AgNPs and the concentration of the bacteria (Mcshan et al. 2015). The effects of co-application ratio however appeared to be strain specific and microalgal-species specific (Fig. 1). In general for MET, CHL and HEX, the 2:1 ratios of *N. oculata*, and the 1.5 ratios of *T. suecica* and *Chlorella* sp. showed higher activities on *B. subtilis*, and *S. uberis*, For *Salmonella* and *K. pneumoniae*, higher activities were exhibited by both ratios, based on the solvent system. Different types of bacteria could develop a quorum sensing (QS) which involves the production and responses to diffusible or secreted signals to modulate its virulence functions and pathogenesis (Abisado et al. 2018). This is a cell-to-cell connection where certain signals are activated to match the pathogenic ways to help bacteria to adapt. Under crowded conditions, the QS signals in bacteria, normally consisting of peptide acyl-homocerin lactone, coordinate the nutrient use and the basic metabolism of individual cells. The antimicrobial resistance to antibiotics or pathogens is a result of the QS signal activation which leads to the formation of biofilm. The development of anti-QS agents can prevent this biofilm formation, thereby reducing the bacterial drug or antibiotic resistance (Hyung et al. 2014; Abisado et al. 2018).

For the G^{-ve} bacteria *Shigella flexneri* and *Pseudomonas aeruginosa*, the significant increase in antibacterial effects is reported for applications of ampicillin with AgNPs, followed by AgNPs–gentamicin, AgNPs–chloramphenicol, AgNPs–erythromycin, AgNPs–tetracycline and AgNPs–vancomycin. There is an improved sensitivity towards G^{+ve} *Staphylococcus aureus* and *Streptococcus pneumoniae* strains, with AgNPs–vancomycin, AgNPs–ampicillin, AgNPs–chloramphenicol, AgNPs–gentamicin, AgNPs–tetracycline, and AgNPs–erythromycin. Ampicillin also exhibits the highest activity against *P. aeruginosa* and *S. flexneri*, with the activities enhanced by the AgNPs co-application (Gurunathan et al. 2014). These synergistic activities of the AgNPs in the presence of different antibiotics suggest that it is possible to kill the pathogenic bacterial cells at lower concentrations of the antibiotics (Barapatre et al. 2016). The anti-bacterial activities can be attributed to the bioactive compounds in the extracts with promising pharmaceutical applications (Matharasi et al. 2018). The ability of the plant or algal extracts in co-application with antibiotic

has the potential to overcome the resistant bacteria even at lower concentration to reduce the side effects (Aiyegoro et al. 2009). The bioactive compounds in the different organic algal extracts may explain the differences in their inhibition zone towards the microbes (Bhagavathy et al. 2011). With the MCEs, the consistent antibacterial activity exhibited by the co-application samples (Additional file 1: Tables S6 and S7) can be attributed to the coordinated and correlative reactions between the active groups of the bioactive compounds or antibiotics, such as the amino groups and hydroxyl, which interact with the large surface area of the AgNPs by chelation (Fayaz et al. 2011). These have added benefits such as providing active features to the food packaging materials with antimicrobial activities, enzyme immobilization, oxygen scavenging ability, or as a signal of the degree of exposure to several degradation-linked factors. The NPs can be utilized to conserve the food from environmental agents, and with combined features to the packaging materials can enhance the foods stability, or suggest their eventual inadequacy to be consumed (De Azeredo 2009).

Conclusion

The study had successfully formulated the new antimicrobial agents against different strains of pathogenic bacteria, based on the AgNPs–MCEs co-application, and carried out the detailed analyses of the extracts from microalgal culture grown over prolonged period, in specific limiting medium such as TMRL. These AgNPs–MCEs formulations as anti-bacterial agents were novel and had not been reported before. The determination of the phytoconstituents showed that the highest lipid was shown by *Chlorella* sp., the highest TSFA was exhibited by *N. oculata*, and followed by *Chlorella* sp., while the *T. suecica* exhibited the highest MUFA and PUFA. The highest carbohydrate and protein contents were recorded in *N. oculata*, the highest TPC in *Chlorella* sp.-CHL, the TFC in *T. suecica*-MET, but the carotenoids levels were comparable in all species. The HPTLC analysis confirmed the presence of EPA and β -carotene in all the MCEs, and based on GC–MS, the major metabolites were 13-docosenamide, (Z)- in *T. suecica*-HEX; phytol in *N. oculata*-HEX; and neophytadiene in *Chlorella* sp.-ETH. The highest antimicrobial activities were shown by the single application of the AgNPs, and the AgNPs–MCEs co-applications exhibited a more stable and consistent activities, as compared to the single MCEs application. The AgNPs–MCEs co-application can therefore be further optimized based on the dosages and the ratios to reduce the side effects, without losing the efficacy. The synergistic effects of the MCEs and the AgNPs in enhancing

the antimicrobial activities pave the way for the AgNPs co-application with the natural products or antibiotics to enhance their activities against different pathogenic and drug-resistant bacteria.

Supplementary information

Supplementary information accompanies this paper at <https://doi.org/10.1186/s40643-020-00322-w>.

Additional file 1. Table S1. Composition of TMRL Enrichment Medium for cultivation of microalgae (AQUACOPs 1984). Table S2. Preparation of AgNPs–MCEs co-application ratio for antimicrobial activity (500 $\mu\text{g}/\text{mL}$). Table S3. The HPTLC parameters of MCEs–CHL for Retention factor (Rf), Area (%) under the curve and Area of Standards (EPA and β -Carotene). Table S4. The HPTLC parameters of MCEs–HEX for Retention factor (Rf), Area (%) under the curve and Area of Standards (EPA and β -Carotene). Table S5. The HPTLC parameters of MCEs–ETH for Retention factor (Rf), Area (%) under the curve and Area of Standards (EPA and β -Carotene). Table S6. Inhibitory effects (mm) of AgNPs and MCEs (500 $\mu\text{g}/\text{mL}$) single application and standard antibiotic penicillin on selected microorganisms for 24 h by using well diffusion methods. The results are expressed as the Means \pm SD of three replicates. Table S7. Inhibitory effects (mm) of AgNPs and MCEs (500 $\mu\text{g}/\text{mL}$) co-application at the 1.5:1 and 2:1 ratios on selected microorganisms for 24 h by using well diffusion methods. The results are expressed as the Means \pm SD of three replicates. Table S8. Minimum inhibitory concentration (MIC, $\mu\text{g}/\text{mL}$) of MCEs and AgNPs single application by using the microtiter plate dilution method. Table S9. Minimum inhibitory concentration (MIC, $\mu\text{g}/\text{mL}$) of AgNPs and MCEs co-application at the 1.5:1 and 2:1 ratios by using the microtiter plate dilution method. Figure S1. Dimensional finger print of the MCEs showing different peaks of phytoconstituents for (a) CHL; (b) HEX; (c) ETH. The identification of β -carotene and EPA in the standards and the MCEs was based on the retention factor (Rf) value as determined by Win CATS software. Figure S2. HPTLC chromatogram of MCEs–CHL extract showing different peaks of phytoconstituents for (a) EPA; (b) β -carotene; (c) *N. oculata*; (d) *T. suecica*; (e) *Chlorella* sp. The identification of β -carotene and EPA in the standards and the MCEs was based on the retention factor (Rf) value as determined by Win CATS software. Figure S3. HPTLC chromatogram of MCEs–HEX extracts showing different peaks of phytoconstituents for (a) EPA; (b) β -carotene; (c) *N. oculata*; (d) *T. suecica*; (e) *Chlorella* sp. The identification of β -carotene and EPA in the standards and the MCEs was based on the retention factor (Rf) value as determined by Win CATS software. Figure S4. HPTLC chromatogram of MCEs–ETH extracts showing different peaks of phytoconstituents for (a) EPA; (b) β -carotene; (c) *N. oculata*; (d) *T. suecica*; (e) *Chlorella* sp. The identification of β -carotene and EPA in the standards and the MCEs was based on the retention factor (Rf) value as determined by Win CATS software. Figure S5. Anti-microbial activity of MCEs and AgNPs single and co-application (1.5:1) against *B. subtilis* for (a) *N. oculata*-MET; (b) *N. oculata*-CHL; (c) *N. oculata*-ETH; (d) *T. suecica*-CHL; (e) *T. suecica*-ETH; (f) *Chlorella* sp.-ETH; (g) AgNPs; (h) Penicillin; (i) AgNPs-*N. oculata*-MET; (j) AgNPs-*N. oculata*-CHL; (k) AgNPs-*T. suecica*-MET; (l) AgNPs-*T. suecica*-CHL; (m) AgNPs-*Chlorella* sp.-MET; (n) AgNPs-*Chlorella* sp.-CHL. Figure S6. Anti-microbial activity of MCEs and AgNPs single and co-application (1.5:1) against *S. uberis* for (a) *N. oculata*-MET; (b) *N. oculata*-CHL; (c) *N. oculata*-ETH; (d) *T. suecica*-ETH; (e) *Chlorella* sp.-CHL; (f) AgNPs; (g) Penicillin; (h) AgNPs-*N. oculata*-MET; (i) AgNPs-*N. oculata*-CHL; (j) AgNPs-*T. suecica*-MET; (k) AgNPs-*T. suecica*-CHL; (l) AgNPs-*Chlorella* sp.-MET; (m) AgNPs-*Chlorella* sp.-CHL. Figure S7. Anti-microbial activity of MCEs and AgNPs single and co-application (1.5:1) against *Salmonella* sp. for (a) *N. oculata*-MET; (b) *N. oculata*-CHL; (c) *N. oculata*-ETH; (d) *T. suecica*-ETH; (e) *Chlorella* sp.-MET; (f) *Chlorella* sp.-CHL; (g) *Chlorella* sp.-ETH; (h) AgNPs; (i) Penicillin; (j) AgNPs-*N. oculata*-MET; (k) AgNPs-*N. oculata*-CHL; (l) AgNPs-*T. suecica*-MET; (m) AgNPs-*T. suecica*-CHL; (n) AgNPs-*Chlorella* sp.-MET; (o) AgNPs-*Chlorella* sp.-CHL. Figure S8. Anti-microbial activity of MCEs and AgNPs single and co-application (1.5:1) against *K. pneumoniae* for (a) *N. oculata*-CHL; (b) *N. oculata*-ETH; (c) *T. suecica*-MET; (d) *T. suecica*-CHL; (e) *Chlorella* sp.-MET; (f) *Chlorella* sp.-CHL; (g) AgNPs; (h) Penicillin; (i)

AgNPs-N. oculata-MET; (j) AgNPs-N. oculata-CHL; (k) AgNPs-T. suecica-MET; (l) AgNPs-T. suecica-CHL; (m) AgNPs-Chlorella sp.-MET; (n) AgNPs-Chlorella sp.-CHL.

Abbreviations

AgNPs: Silver nanoparticles; MCEs: Microalgal crude extracts; ROS: Reactive oxygen species; HPTLC: High-performance thin-layer chromatography; GC-MS: Gas chromatography-mass spectrometry; MET: Methanol; ETH: Ethanol; CHL: Chloroform; HEX: Hexane; W: Water; TSFA: Total saturated fatty acids; MUFA: Monounsaturated fatty acids; PUFA: Polyunsaturated fatty acids; EPA: Eicosapentaenoic acid; TPC: Total phenolics content; TFC: Total flavonoids content.

Acknowledgements

The authors thank the Science Officers in the Institute of Marine Biotechnology, Universiti Malaysia Terengganu for their assistance with the facilities.

Authors' contributions

HAH: investigation, methodology, data curation, formal analysis, writing—original draft; DFS, SAMR, JYFS, NAMZ: resources; MAA: conceptualization, funding acquisition, project administration, supervision, writing—review and editing. All authors read and approved the final manuscript.

Funding

This research was partially funded by the Fundamental Research Grant Scheme, Ministry of Higher Education, Malaysia under FRGS/1/2015/SG05/UMT/02/4.

Availability of data and materials

The data and materials will be made available upon request.

Ethical approval and consent to participate

Not applicable.

Consent for publication

All authors have consented to the publication of the manuscript.

Competing interests

There are no competing interests to declare.

Author details

¹ Institute of Marine Biotechnology, Universiti Malaysia Terengganu, 21030 Kuala Nerus, Terengganu, Malaysia. ² College of Dentistry, University of Basrah, 00964 Basrah, Iraq.

Received: 30 March 2020 Accepted: 16 June 2020

Published online: 15 July 2020

References

- Abdullah MA, Ahmad A, Shah SMU, Shanab SMM, Ali HEA, Abo-State MAM, Othman MF (2016) Integrated algal engineering for bioenergy generation, effluent remediation, and production of high-value bioactive compounds. *Biotechnol Bioprocess Eng* 21:236–249
- Abisado RG, Benomar S, Klaus JR, Dandekar AA, Chandler JR (2018) Bacterial quorum sensing and microbial community interactions. *mBio* 9:e01749–e01818. <https://doi.org/10.1128/mBio.01749-18>
- Agoramoorthy G, Chandrasekaran M, Venkatesalu V, Hsu MJ (2007) Antibacterial and antifungal activities of fatty acid methyl esters of the blind your eye mangrove from India. *Braz J Microbiol* 38:739–742
- Ahmad A, Shah SMU, Othman MF, Abdullah MA (2014) Enhanced palm oil mill effluent treatment and biomethane production by co-digestion of oil palm empty fruit bunches with *Chlorella* sp. *Can J Chem Eng* 92:1636–1642
- Ahmad A, Shah SMU, Othman MF, Abdullah MA (2015) Aerobic and anaerobic co-cultivation of nannochloropsis oculata with oil palm empty fruit bunch for enhanced biomethane production and palm oil mill effluent treatment. *Desalin Water Treat* 56:2055–2065
- Aiyegoro OA, Okoh AI (2010) Preliminary phytochemical screening and in vitro antioxidant activities of the aqueous extract of *Helichrysum longifolium* DC. *BMC Compl Altern Med* 10:21
- Aiyegoro OA, Afolayan AJ, Okoh AI (2009) In vitro antibacterial activities of crude extracts of the leaves of *Helichrysum longifolium* in combination with selected antibiotics. *Afr J Pharm Pharmacol* 3:293–300
- Alam P (2013) Densitometric HPTLC analysis of 8-gingerol in Zingiber officinale extract and ginger-containing dietary supplements, teas and commercial creams. *Asian Pac J Trop Biomed* 3:634–638
- Alonso Á, Belarbi E, Ferna ÁM, Lo D, Rodríguez-ruiz J, Grima EM (2000) Acyl lipid composition variation related to culture age and nitrogen concentration in continuous culture of the microalga *Phaeodactylum tricornutum*. *Phytochemistry* 54:461–471
- Al-saif SSA, Abdel-raouf N, El-Wazanani HA, Aref IA (2014) Antibacterial substances from marine algae isolated from Jeddah coast of Red sea, Saudi Arabia. *Saudi J Biol Sci* 21:57–64
- Alsufyani T (2014) Metabolite profiling of the chemosphere of the macroalga *Ulva* (Ulvales, Chlorophyta) and its associated bacteria. PhD dissertation, Thüringer Universitäts- und Landesbibliothek Jena, pp 1–210
- Amaro HM, Guedes AC, Malcata FX (2011) Antimicrobial activities of microalgae: an invited review. *Sci Microb Pathog Commun Curr Res Technol Adv* 3:1272–1284
- Amarowicz R (2009) Squalene: a natural antioxidant? *Eur J Lipid Sci Technol* 111:411–412
- AQUACOPs (1984) Review of ten years of experimental penaeid shrimp culture in Tahiti and New Caledonia (South Pacific). *J World Maric Soc* 15:73–91
- Arisz SA, Van Himbergen JAJ, Musgrave A, Van Den Ende H, Munnik T (2000) Polar glycerolipids of *Chlamydomonas moewusii*. *Phytochemistry* 53:265–270
- Arnon DI (1949) Copper enzymes in isolated chloroplasts. *Polyphenoloxidase in Beta vulgaris*. *Plant Physiol* 24:1
- Azim NH, Subki A, Yusof ZNB (2018) Abiotic stresses induce total phenolic, total flavonoid and antioxidant properties in Malaysian indigenous microalgae and cyanobacterium. *Malays J Microbiol* 14:25–33
- Balaji M, Thamilsivan D, Vinayagam SC, Balakumar BS (2017) Anticancer, antioxidant activity and GC-MS analysis of selected micro algal members of chlorophyceae. *Int J Pharm Sci Res* 8:3302–3314
- Balamurugan M, Selvam GG, Thinakaran T, Sivakumar K (2014) Biochemical study and GC-MS analysis of *Hypnea musciformis* (Wulf.) Lamouroux. *Am J Sci Res* 8:117–123
- Barapatre A, Aadil KR, Jha H (2016) Synergistic antibacterial and antibiofilm activity of silver nanoparticles biosynthesized by lignin-degrading fungus. *Bioresour Bioprocess* 3:8
- Becker EW (2007) Micro-algae as a source of protein. *Biotechnol Adv* 25:207–210
- Bhagavathy S, Sumathi P, Bell IJS (2011) Green algae *Chlorococcum humicola*—a new source of bioactive compounds with antimicrobial activity. *Asian Pac J Trop Biomed* 1:S1–S7
- Bhattacharjee M (2016) Pharmaceutically valuable bioactive compounds of algae. *Asian J Pharm Clin Res* 9:43
- Blake KL, O'Neill AJ (2013) Transposon library screening for identification of genetic loci participating in intrinsic susceptibility and acquired resistance to antistaphylococcal agents. *J Antimicrob Chemother* 68:12–16
- Bligh EG, Dyer WJ (1959) A rapid method of total lipid extraction and purification. *Can J Biochem Physiol* 37:911–917
- Brown MR (1991) The amino-acid and sugar composition of 16 species of microalgae used in mariculture. *Exp Mar Biol Ecol* 145:79–99
- Carballo-Cárdenas EC, Tuan PM, Janssen M, Wijffels RH (2003) Vitamin E (α -tocopherol) production by the marine microalgae *Dunaliella tertiolecta* and *Tetraselmis suecica* in batch cultivation. *Biomol Eng* 20:139–147
- Chaudhari BG, Patel NM, Shah PB, Modi KP (2006) Development and validation of a HPTLC method for the simultaneous estimation of atorvastatin calcium and ezetimibe. *Indian J Pharm Sci* 68:793–796
- Cubas C, Lobo MG, González M (2008) Optimization of the extraction of chlorophylls in green beans (*Phaseolus vulgaris* L.) by N, N-dimethylformamide using response surface methodology. *J Food Compos Anal* 21:125–133
- Das R, Gang S, Nath SS (2011) Preparation and Antibacterial Activity of Silver Nanoparticles. *J Biomater Nanobiotechnol* 2:472–475

- De Azeredo HMC (2009) Nanocomposites for food packaging applications. *Food Res Int* 42:1240–1253
- Dere Ş, Güneş T, Sivaci R (1998) Spectrophotometric determination of chlorophyll-A, B and total carotenoid contents of some algae species using different solvents. *Turk J Botany* 22:13–18
- Dineshkumar R, Narendran R, Jayasingam P, Sampathkumar P (2017) Cultivation and chemical composition of microalgae *Chlorella vulgaris* and its antibacterial activity against human pathogens. *J Aquac Mar Biol* 5:00119
- Do QD, Angkawijaya AE, Tran-Nguyen PL, Huynh LH, Soetaredjo FE, Ismadji S, Ju YH (2014) Effect of extraction solvent on total phenol content, total flavonoid content, and antioxidant activity of *Limnophila aromatica*. *J Food Drug Anal* 22:296–302
- Ebrahimzadeh MA, Khalili M, Dehpour AA (2018) Antioxidant activity of ethyl acetate and methanolic extracts of two marine algae, *Nannochloropsis oculata* and *Gracilaria gracilis*—an in vitro assay. *Brazilian J Pharm Sci* 54:e17280
- Farvin KHS, Jacobsen C (2013) Phenolic compounds and antioxidant activities of selected species of seaweeds from Danish coast. *Food Chem* 138:1670–1681
- Fayaz AM, Girilal M, Rahman M, Venkatesan R, Kalaichelvan PT (2011) Biosynthesis of silver and gold nanoparticles using thermophilic bacterium *Geobacillus stearothermophilus*. *Process Biochem* 46:1958–1962
- Goiris K, Muylaert K, Fraeye I, Foubert I, De Brabanter J, De Cooman L (2012) Antioxidant potential of microalgae in relation to their phenolic and carotenoid content. *J Appl Phycol* 24:1477–1486
- Gonzalez LE, Bashan Y (2000) Increased growth of the microalga *Chlorella vulgaris* when coimmobilized and cocultured in alginate beads with the plant-growth-promoting bacterium *Azospirillum brasilense*. *Appl Environ Microbiol* 66:1527–1531
- Gouveia L, Oliveira AC (2009) Microalgae as a raw material for biofuels production. *J Ind Microbiol Biotechnol* 36:269–274
- Gu N, Lin Q, Li G, Tan Y, Huang L, Lin J (2012) Effect of salinity on growth, biochemical composition, and lipid productivity of *Nannochloropsis oculata* CS 179. *Eng Life Sci* 12:631–637
- Guldhe A, Misra R, Singh P, Rawat I, Bux F (2016) An innovative electrochemical process to alleviate the challenges for harvesting of small size microalgae by using non-sacrificial carbon electrodes. *Algal Res* 19:292–298
- Gurunathan S, Han JW, Kwon DN, Kim JH (2014) Enhanced antibacterial and anti-biofilm activities of silver nanoparticles against Gram-negative and Gram-positive bacteria. *Nanoscale Res Lett* 9:373
- Gwo J, Chiu J, Chou C, Cheng H (2005) Cryopreservation of a marine microalga, *Nannochloropsis oculata* (Eustigmatophyceae). *Cryobiology* 50:338–343
- Hafsa MBEN, Ismail MBEN, Garrab M, Aly R, Gagnon J, Naghmouchi K (2017) Antimicrobial, antioxidant, cytotoxic and anticholinesterase activities of water-soluble polysaccharides extracted from microalgae *Isochrysis galbana* and *Nannochloropsis oculata*. *J Serbian Chem Soc* 82:509–522
- Humphrey AM (1980) Chlorophyll. *Food Chem* 5:57–67
- Hussein HA, Mohamad H, Ghazaly MM, Laith AA, Abdullah MA (2020a) Cytotoxic effects of *Tetraselmis suecica* chloroform extracts with silver nanoparticle co-application on MCF-7, 4T1, and Vero cell lines. *J Appl Phycol* 32:127–143
- Hussein HA, Mohamad H, Ghazaly MM, Laith AA, Abdullah MA (2020b) Cytotoxic and antioxidant activities of *Nannochloropsis oculata* and *Chlorella* sp. extracts with silver nanoparticle co-applications. *J King Saud Univ Sci* (JKSUS-D-20-00531 - Under review)
- Hynstova V, Sterbova D, Klejbus B, Hedbavny J, Huska D, Adam V (2017) Separation, identification and quantification of carotenoids and chlorophylls in dietary supplements containing *Chlorella vulgaris* and *Spirulina platensis* using high performance thin layer chromatography. *J Pharm Biomed Anal* 148:108–118
- Hyung J, Goo E, Kim H, Seo Y, Hwang I (2014) Bacterial quorum sensing and metabolic slowing in a cooperative population. *Proc Natl Acad Sci USA* 111:1412–1417
- Ibañez E, Herrero M, Mendiola JA, Castro-Puyana M (2012) Extraction and characterization of bioactive compounds with health benefits from marine resources: macro and micro algae, cyanobacteria, and invertebrates. *Mar Bioact Compd*. Springer, Boston, pp. 55–98
- Irianto A, Austin B (2002) Probiotics in aquaculture. *J Fish Dis* 25:633–642
- Jayshree A, Jayashree S, Thangaraju N (2016) *Chlorella vulgaris* and *Chlamydomonas reinhardtii*: effective antioxidant, antibacterial and anticancer mediators. *Indian J Pharm Sci* 78:575–581
- Jeffrey SW, Mantoura RFC, Wright SW (eds) (1997) *Phytoplankton pigments in oceanography: guidelines to modern methods*. UNESCO Publishing, Paris, pp 37–39
- Kannan RRR, Arumugam R, Anantharaman P (2010) Antibacterial potential of three seagrasses against human pathogens. *Asian Pac J Trop Med* 3:890–893
- Kapoor RV (2014) Mass spectrometry based hyphenated techniques for microalgal and mammalian metabolomics. PhD dissertation, University of Sheffield, pp 1–381
- Kirk JTO, Allen RL (1965) Dependence of chloroplast pigment synthesis on protein synthesis: effect of actidione. *Biochem Biophys Res Commun* 21:523–530
- Kowalska T, Sherma J (2006) *Preparative layer chromatography*. CRC Press, pp 1–423
- Kumaradevan G, Damodaran R, Mani P, Dineshkumar G, Jayaseelan T (2015) Phytochemical screening and GC-MS analysis of bioactive components of ethanolic leaves extract of *Clerodendrum phlomidis* (L.). *Am J Biol Pharm Res* 2:142–148
- Maadane A, Merghoub N, Ainane T, El Arroussi H, Benhima R, Amzazi S et al (2015) Antioxidant activity of some Moroccan marine microalgae: pufa profiles, carotenoids and phenolic content. *J Biotechnol* 215:13–19
- Maadane A, Merghoub N, El Mernissi N, Ainane T, Amzazi S, Wahby I, Bakri Y (2017) Antimicrobial activity of marine microalgae isolated from Moroccan coastlines. *J Microbiol Biotechnol Food Sci* 6:1257–1260
- Mata TM, Martins AA, Caetano NS (2010) Microalgae for biodiesel production and other applications: a review. *Renew Sustain Energy Rev* 14:217–232
- Matharasi A, Kumar RD, Prabakaran G, Kumar PS (2018) Phytochemical screening and antimicrobial activity of marine microalgae *Tetraselmis* sp. *Int J Pharm Biol Sci* 8:85–90
- Mcshan D, Zhang Y, Deng H, Ray PC, Yu H (2015) Synergistic antibacterial effect of silver nanoparticles combined with ineffective antibiotics on drug resistant *Salmonella typhimurium* DT104. *J Environ Sci Heal Part C* 33:369–384
- Murugesan S, Bhuvanewari S (2016) HPTLC fingerprint profile of methanol extract of the marine red alga *Portieria hornemannii* (Lyngbye) (Silva). *Int J Adv Pharm* 5:10–14
- Natarajan K, Selvaraj S, Murty VR (2010) Microbial production of silver nanoparticles. *Dig J Nanomater Biostructures* 5:135–140
- Oo YYN, Su MC, Kyaw KT (2017) Extraction and determination of chlorophyll content from microalgae. *Int J Adv Res Publ* 1:298–301
- Otari SV, Patil RM, Nadaf NH, Ghosh SJ, Pawar SH (2014) Green synthesis of silver nanoparticles by microorganism using organic pollutant: its antimicrobial and catalytic application. *Env Sci Pollut Res* 21:1503–1513
- Pal S, Tak YK, Song JM (2007) Does the antibacterial activity of silver nanoparticles depend on the shape of the nanoparticle? A study of the gram-negative bacterium *Escherichia coli*. *Appl Environ Microbiol* 73:1712–1720
- Pandithurai M, Murugesan S, Sivamurugan V, Lakshmisundaram R (2015) Chromatographic fingerprint analysis of *Spatoglossum asperum* J. Agardh by HPTLC Technique. *Am J Mod Chromatogr* 2:7–15
- Pengov A, Ceru S (2003) Antimicrobial drug susceptibility of *Staphylococcus aureus* strains isolated from bovine and ovine mammary glands. *J Dairy Sci* 86:3157–3163
- Pérez-lópez P, González-garcía S, Ulloa RG, Sineiro J, Feijoo G, Moreira MT (2014) Life cycle assessment of the production of bioactive compounds from *Tetraselmis suecica* at pilot scale. *J Clean Prod* 64:323–331
- Puong TV, Lam PVH, Diep CN (2018) Bioactive compounds from marine *Streptomyces* sp. by gas chromatography-mass. *Pharm Chem J* 5:196–203
- Picardo MC, de Medeiros JL, de Araújo O, Chaloub RM (2013) Bioresource technology effects of CO₂ enrichment and nutrients supply intermittency on batch cultures of *Isochrysis galbana*. *Bioresour Technol* 143:242–250
- Rajendran N, Karpanai Selvan B, Sobana Piriya P, Logeswari V, Kathiresan E, Tamilselvi A, John Vennison S (2014) Phytochemicals, antimicrobial and antioxidant screening from five different marine microalgae. *J Chem Pharm Sci* 78–85
- Rajeshkumar S, Malarkodi C (2014) In vitro antibacterial activity and mechanism of silver nanoparticles against foodborne pathogens. *Bioinorg Chem Appl* 2014:10

- Rao AR, Dayananda C, Sarada R, Shamala TR, Ravishankar GA (2007) Effect of salinity on growth of green alga *Botryococcus braunii* and its constituents. *Bioresour Technol* 98:560–564
- Safafar H, Uldall Nørregaard P, Ljubic A, Møller P, Løvstad Holdt S, Jacobsen C (2016) Enhancement of protein and pigment content in two *Chlorella* species cultivated on industrial process water. *J Mar Sci Eng* 4:84
- Sangeetha P, Suganya V, Bhuvana P, Anuradha V, Ali MS (2018) Physicochemical characterization and drug standardization of *Nannochloropsis oculata*. *Worlds J Pharm Med Res* 4:167–171
- Servaites JC, Faeth JL, Sidhu SS (2012) A dye binding method for measurement of total protein in microalgae. *Anal Biochem* 421:75–80
- Servel MO, Claire C, Derrien A, Coiffard L, Roeck-Holtzhauer DE (1994) Fatty acid composition of some marine microalgae. *Phycochemistry* 36:691–693
- Shah SMU (2014) Cell culture optimization and reactor studies of green and brown microalgae for enhanced lipid production. PhD dissertation, Universiti Teknologi PETRONAS, Seri Iskandar, Malaysia
- Shah SMU, Abdullah MA (2018) Effects of macro/micronutrients on green and brown microalgal cell growth and fatty acids in photobioreactor and open-tank systems. *Biocatal Agric Biotechnol* 14:10–17
- Shah SMU, Ahmad A, Othman MF, Abdullah MA (2016) Effects of palm oil mill effluent media on cell growth and lipid content of *Nannochloropsis oculata* and *Tetraselmis suecica*. *Int J Green Energy* 13:200–207
- Shannon E, Abu-ghannam N (2016) Antibacterial derivatives of marine algae: an overview of pharmacological mechanisms and applications. *Mar Drugs* 14:81
- Silhavy T, Kahne D, Walker S (2010) The bacterial cell envelope. *Cold Spring Harb Perspect Biol* 2:a000414
- Siripatrawan U, Harte BR (2010) Physical properties and antioxidant activity of an active film from chitosan incorporated with green tea extract. *Food Hydrocoll* 24:770–775
- Sivasubramanian R, Brindha P (2013) In-vitro cytotoxic, antioxidant and GC–MS studies on *Centrathium punctatum* Cass. *Int J Pharm Pharm Sci* 5:364–367
- Smith VJ, Desbois AP, Dyrzynda EA (2010) Conventional and unconventional antimicrobials from fish, marine invertebrates and micro-algae. *Mar Drugs* 8:1213–1262
- Soliman H, Elsayed A, Dyaa A (2018) Antimicrobial activity of silver nanoparticles biosynthesized by *Rhodotorula* sp. strain ATL72. *Egypt J Basic Appl Sci* 5:228–233
- Songisepp E, Kullisaar T, Hütt P, Elias P, Brilene T, Zilmer M, Mikelsaar M (2004) A new probiotic cheese with antioxidative and antimicrobial activity. *J Dairy Sci* 87:2017–2023
- Sunita A, Manju S (2017) Phytochemical examination and GC–MS analysis of methanol and ethyl-acetate extract of root and stem of *Gisekia Pharmaceoides* Linn. *Res J Pharm Biol Chem Sci* 8:168–174
- Sunita P, Sivaraj R, Venkatesh R, Vanathi P, Vanathi P, Rajiv P (2015) Anticancer potential of green synthesized silver nanoparticles: a review. *Int J Curr Res* 7:21539–21544
- Sushma GS, Devi BA, Madhulatha CH, Kumar KU, Harathi P, Subramanian NS, Ramadevi M (2013) Preliminary phytochemical screening and HPTLC fingerprinting of leaf extracts of *Ficus nervosa* Heyne ex Roth. *J Chem Pharm Res* 5:98–104
- Swamy MK, Sinniah UR (2015) A comprehensive review on the phytochemical constituents and pharmacological activities of *Pogostemon cablin* Benth.: an aromatic medicinal plant of industrial importance. *Molecules* 20:8521–8547
- Talib WH, Abu Zarga MH, Mahasneh AM (2012) Antiproliferative, antimicrobial and apoptosis inducing effects of compounds isolated from *Inula viscosa*. *Molecules* 17:3291–3303
- Thennarasan S, Murugesan S, Subha TS (2014) HPTLC finger printing profile of brown alga *Lobophora variegata*. *J Chem Pharm Res* 6:674–677
- Velusamy P, Kumar GV, Jeyanthi V, Das J, Pachiappan R (2016) Bio-inspired green nanoparticles: synthesis, mechanism, and antibacterial application. *Toxicol Res* 32:95–102
- Venkara Raman B, Samuel LA, Pardha Saradhi M, Narashimha Rao B, Naga Vamsi Krishna A, Sudhakar M, Radhakrishnan TM (2012) Antibacterial, antioxidant activity and GC-MS analysis of *Eupatorium odoratum*. *Asian J Pharm Clin Res* 5:99–106
- Wang T, Jónsdóttir R, Ólafsdóttir G (2009) Total phenolic compounds, radical scavenging and metal chelation of extracts from Icelandic seaweeds. *Food Chem* 116:240–248
- Wei LS, Wee W, Siong JYF, Syamsumir DF (2011) Characterization of anticancer, antimicrobial, antioxidant properties and chemical compositions of *Peperomia pellucida* leaf extract. *Acta Med Iran* 49:670–674
- Widowati I, Zainuri M, Kusumaningrum HP, Susilowati R, Hardivillier Y, Leignel V, et al. (2017) Antioxidant activity of three microalgae *Dunaliella salina*, *Tetraselmis chunii* and clone Tahiti. In IOP Conf. Ser. Earth Environ. Sci. *Isochrysis galbana*, vol. 55. IOP Publishing, pp. 012067.
- Wu LC, Ho JAA, Shieh MC, Lu LW (2005) Antioxidant and antiproliferative activities of *Spirulina* and *Chlorella* water extracts. *J Agric Food Chem* 53:4207–4212
- Yadavalli R, Peasari JR, Mamindla P, Praveenkumar Mounika S, Ganugapati J (2018) Phytochemical screening and in silico studies of flavonoids from *Chlorella pyrenoidosa*. *Inf Med Unlocked* 10:89–99
- Yao L, Gerde JA, Lee S, Wang T, Harrata AK (2015) Microalgae lipid characterization. *J Agric Food Chem* 63:1773–1787
- Young AJ, Britton G (2012) Carotenoids in photosynthesis. Springer, Berlin, pp. 72–95
- Yu FR, Lian XZ, Guo HY, McGuire PM, Li RD, Wang R, Yu FH (2005) Isolation and characterization of methyl esters and derivatives from *Euphorbia kansui* (Euphorbiaceae) and their inhibitory effects on the human SGC-7901 cells. *Pharm Pharm Sci* 8:528–535
- Zittelli GC, Rodolfi L, Biondi N, Tredici MR (2006) Productivity and photosynthetic efficiency of outdoor cultures of *Tetraselmis suecica* in annular columns. *Aquaculture* 261:932–943

Publisher's Note

Springer Nature remains neutral with regard to jurisdictional claims in published maps and institutional affiliations.

Submit your manuscript to a SpringerOpen® journal and benefit from:

- Convenient online submission
- Rigorous peer review
- Open access: articles freely available online
- High visibility within the field
- Retaining the copyright to your article

Submit your next manuscript at ► [springeropen.com](https://www.springeropen.com)